THE JOURNAL OF PHYSICAL CHEMISTRY B

Article

pubs.acs.org/JPCB

Molecular Strategies to Achieve Selective Conductance in NaK Channel Variants

Yibo Wang,[†] Adam C. Chamberlin,[†] and Sergei Yu. Noskov*

Centre for Molecular Simulation, Department of Biological Sciences, University of Calgary 2500 University Drive, Calgary, Alberta, Canada, T2N 1N4

Supporting Information

ABSTRACT: A recent crystallization of several ion channels has provided strong impetus for efforts aimed at understanding the different strategies employed by nature for selective ion transport. In this work, we used two variants of the selectivity filter of NaK channel to explore molecular mechanisms that give rise to K^+-selectivity. We computed one-dimensional (1D) and two-dimensional (2D) potentials of mean force (PMFs) for ion permeation across the channel. The results indicate that the energies for Na^+ and K^+ permeation across the selectivity filter display significant differences in positions of the binding sites and barriers. One characteristic signature of a K^+-selective channel is the apparent preservation of the site analogous to that of S2 in KcsA. The S2-bound ion can be almost ideally dehydrated and coordinated by 6 to 8 carbonyls. In a striking contrast, the PMFs controlling transport of ions in a nonselective variant show almost identical profiles for either K^+ or Na^+ and significant involvement of water molecules in ion coordination across the entire selectivity filter. An analysis of differences in 1D PMFs for Na^+ and K^+ suggests that coordination number alone is an insufficient predictor of site selectivity, while chemical composition (ratio of carbonyls and water molecules) correlates well with preference for K^+. Multi-ion effects such as dependence of the barriers and wells for permeant ion on the type of copermeant ion were found to play a significant role in the selectivity signature of the channel as well.

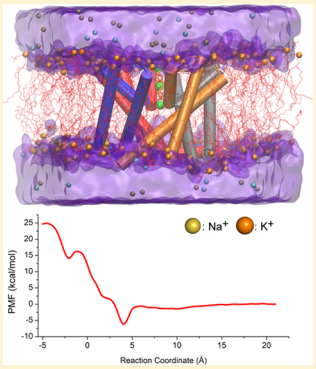

INTRODUCTION

Ion channels are integral membrane proteins involved in selective or nonselective ion transport in response to external stimuli such as changes in membrane voltage and osmotic pressure or binding of a ligand. They play pivotal roles in pacemaking, neuronal signaling, and smooth muscle function and are major targets for drug development.[1,2] One of the most studied and debated properties of ion-selective channels is their ability to discriminate between similar ions (Na^+ vs K^+) and yet transport ions even near diffusion limits.[3] The mechanism of selectivity has been studied for decades and significant progress has been made in understanding selective transport in channels and transporters.[3−9] However, the mechanism of selectivity in the filter remains to be understood. The first crystal structure of bacterial K^+-selective channel KcsA reported in 1998 provided strong momentum for studies of selective transport.[10−16] Most of the K^+-selective channels display a highly conserved amino acid sequence TVGYG in the selectivity filter, which forms the selective permeation pathway for K^+ and discriminates against competing Na^+ ions. This TVGYG motif forms four continuous binding sites labeled as S1, S2, S3, and S4, respectively. It has been well established that ions can also stably bind to the extracellular site S0[13] or reside in an intracellular cavity site stabilized by pore helix macrodipoles.[17] Most of the ion binding sites in the selectivity filter of K-selective channels are composed of main-chain oxygen atoms forming 8-atom twisted-cube coordination cages for permeating K^+ ions and/or water molecules and 6-atom octahedral coordination cages for Na^+.[10,11,18,19] Prior work led us to conclude that the binding-site composition (type and number of coordinating ligands) is sufficient to explain the free-energy difference in binding between competing ions in the presence of thermodynamic fluctuations.[20−23] Several other mechanisms for selective conductance have been proposed, emphasizing the importance of matching coordination states available to an ion in a bulk phase with the coordination mode observed in the protein binding sites.[24−31] Analysis of multi-ion potentials of mean force (PMFs) for ion transport across the KcsA selectivity filter underscored the importance of kinetic factors in selective conductance across K^+ channels such as KcsA.[32]

The NaK channel[33,34] has a very similar selectivity filter sequence, TVGDG, yet lacks selectivity for either K^+ or Na^+. This channel may serve as an excellent negative control for the different mechanisms proposed. Noskov and Roux,[20] focusing primarily on the thermodynamics of ion binding to nonselective filter of NaK, showed that the differences in hydration of the cations may be responsible for the loss of Na/K selectivity in the NaK channel. In 2011, Derebe et al.[35] engineered the filter of the NaK channel to have either K^+-selective or nonselective mutant. They found that the selectivity of the mutant channel displays a clear dependence on the number of binding sites in the selectivity filter and postulated

Received: October 31, 2013
Revised: February 6, 2014
Published: February 7, 2014

dx.doi.org/10.1021/jp4107537 | J. Phys. Chem. B 2014, 118, 2041−2049

that kinetic effects play a significant role in the emergence of ion-selective transport. High-resolution X-ray structures display three (nonselective channel NaK2CNG with TVGDTP in the filter) or four (highly K^+-selective channel NaK2K with TVGYGD in the filter) binding sites (Figure 1A, B).[35] The

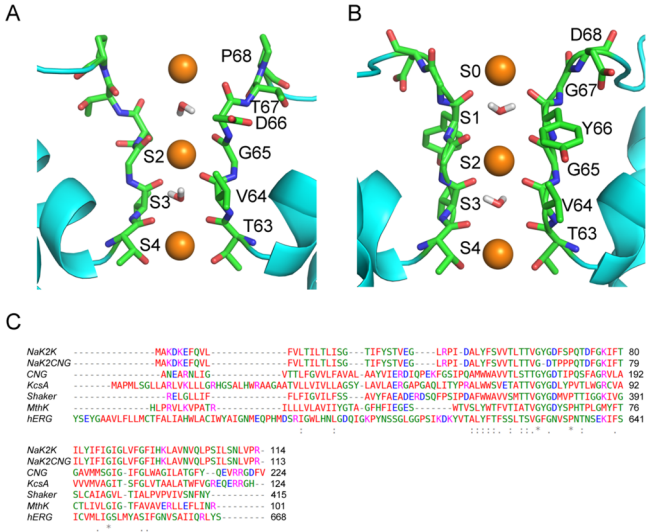

Figure 1. Structure of the selectivity filter with the binding sites of: (A) NaK2CNG and (B) NaK2K. (C) The pore domain sequence alignment shows NaK2K (3OUF) with NaK2CNG (3K03), as well as CNG (3BEH), KcsA (1K4C), Shaker (3LUT), MthK (4HYO), and hERG for comparison.

sequence alignment of NaK and its variants with other channels (Figure 1C) shows that NaK and its variants may provide an indispensable platform for understanding ion transport across K^+ selective and nonselective channels of great clinical importance, such as HCN or EAG channels. The selective channel NaK2K displays a permeability ratio ($P_{Na}{}^+/P_{K}{}^+$) of about 0.04 with a single channel conductance of ~120 pS. Interestingly, NaK2K is Na^+ permeable with a low conductance of ~10 pS in the absence of K^+, and the phenomena also reported for hERG channels.[36] NaK2CNG is a nonselective channel with a single channel conductance of ~110 pS.[35] The conductivity and selectivity mechanisms remain controversial. To learn more about the emergence of K^+-selectivity in NaK variants, we used all-atom molecular dynamics (MD) simulations with an explicit membrane to determine the multi-ion PMFs corresponding to the entry of Na^+ or K^+ into the selectivity filter assuming two-ion occupancy following the protocol presented by Egwolf and Roux.[3] The PMF decomposition allows us to investigate the role played by coordination states and composition of the binding site for a given ion, as well as to understand why the addition of a fourth site is critical for Na^+/K^+ selectivity.

METHODS

The atomic coordinates and structure factors of the NaK2CNG and NaK2K were obtained from the Protein Data Bank (PDB ID: 3K03 for NaK2CNG and 3OUF for NaK2K).[35] The homotetramers were embedded in the DMPC bilayer lipids with the permeation pathway aligned along the z-axis using the CHARMM-GUI membrane builder protocol.[37] The systems were solvated in ~7500 TIP3P water molecules with 150 mM KCl in an 84 × 84 × 73 $Å^3$ box. These systems were simulated with the CHARMM c36 package,[38] using the CHARMM PARAM27 force field for all nonionic compounds.[39,40] However, the force field parameters for ions were chosen in accordance with Noskov and Roux, which correlates with experimental binding energies.[41] The parameters were optimized to give a relative free energy difference in TIP3P water ΔG = 18.12 kcal/mol between Na^+ and K^+. The exact parameters including Lennard-Jones parameters and NBFIX corrections for ion-carbonyl interactions were published previously in a supplement to ref 41. The NpAT (constant area) ensemble with Hoover thermostat was used for all the simulations with pressure at 1 atm and temperature at 315 K.[42] Nonbonded interactions were switched off at 10−12 Å and long-range electrostatic interactions were treated by the Particle Mesh Ewald (PME) algorithm.[43] The time step was 1 fs with the SHAKE algorithm being used.[44] Following a staged equilibration with a gradual decrease in harmonic constraints on heavy protein atoms only, further nonconstrained equilibrations were run for 10 ns.

Free energy profiles, PMFs for example, for ion permeation were calculated by one-dimensional (1D) and two-dimensional (2D) umbrella sampling methods, a powerful computational technique used with considerable success in studies of K-channels.[3,45] In this paper, only the transport of ions from the extracellular bulk to the cavity of the channel was considered because of the tendency of the gate to close during the transport from the cavity to the intracellular solution. Umbrella sampling simulations were performed with harmonic biasing potentials with a force constant of 10 kcal/(mol·$Å^2$) along the z-axis. The zero position along the z-axis is the center of mass (COM) of the backbone atoms of residues 63−66 in the filter. The reaction coordinate for each ion was the distance along the z-axis between the ion and the zero position. Snapshots of the conventional MD simulations were employed as the starting conformations for the umbrella sampling. The sampling windows were spaced every 0.5 Å from −15.0 Å to 15.0 Å resulting in 61 windows for 1D single-ion PMF computations. For 2D multi-ion PMFs, the reaction coordinates were the distance along the z-axis between the outer ion and the zero position (z_1) and the distance along the z-axis between the COM of the inner two ions and the zero position (z_{23}). The windows were spaced from −6.0 Å to 20.0 Å for the outer ion and from −12.0 Å to 15.0 Å for the center of the other two inner ions with a total of 1540 windows. Considering the diameter of the filter is about 3 Å while the ionic radius is 1.39 Å for K^+ and 1.02 Å for Na^+, ions changing positions are highly improbable and so only the scenario where the ions to pass through the filter one by one was investigated. The simulation time per window was set to 1 ns for 1D single-ion PMF computations and 200 ps for 2D multi-ion PMF computations. The energy surfaces were rebuilt using the weighted histogram analysis method (WHAM).[46,47] The tolerance for WHAM was set to 0.001.

Kramer's Rate describes the escape rate of the system from a stable state to another state.[48,49] Kramer's Rate is estimated by

$$\text{rate} = \frac{D\sqrt{K_b K_w}}{2\pi k_B T} \exp\left(\frac{-\Delta W}{k_B T}\right)$$

where D is the approximate ionic diffusion coefficient and in this case we used 0.001 $Å^2$/ps.[32,50] ΔW is the free energy difference between the barrier and the well. K_b and K_w are the curvatures of the barrier and well, respectively.[32]

dx.doi.org/10.1021/jp4107537 | J. Phys. Chem. B 2014, 118, 2041−2049

The equilibrium dissociation constant K_D(single) for the binding of K^+ or Na^+ from 1D single-ion PMF in the presence of a cylindrical constraint can be expressed as follows[32,51]

$$K_D^{-1}(\text{single}) = \pi R^2 \int_{z_{min}}^{z_{max}} dz\ e^{-w(z)/k_BT}$$

where R is the radius of the cylindrical restraint and is oriented normal to the z-axis with $z_{min} = -15$ Å and $z_{max} = 15$ Å. The $w(z)$ was offset to zero when the ion was in the bulk.

Similarly, the equilibrium dissociation constant of a multiple occupancy state of the channel, K_D(multiple), can be expressed as[51,52]

$$K_D^{-1}(\text{multiple}) = \frac{(\pi^2R^4)\int_{z_{1,min}}^{z_{1,max}} dz_1 \int_{z_{23,min}}^{z_{23,max}} dz_{23}\ e^{-w(z_1,z_{23})/k_BT}}{\pi R^2 \int_{z_{min}}^{z_{max}} dz\ e^{-w(z)/k_BT}}$$

with the following limits of integration: -6.0 Å $\le z_1 \le 21.0$ Å and -12.0 Å $\le z_{23} \le 15.0$ Å.

RESULTS AND DISCUSSIONS

Potentials of Mean Force for Ion Permeation across the NaK2CNG Channel. The free-energy profiles for NaK2CNG with K^+ and Na^+ are shown in Figure 2. All

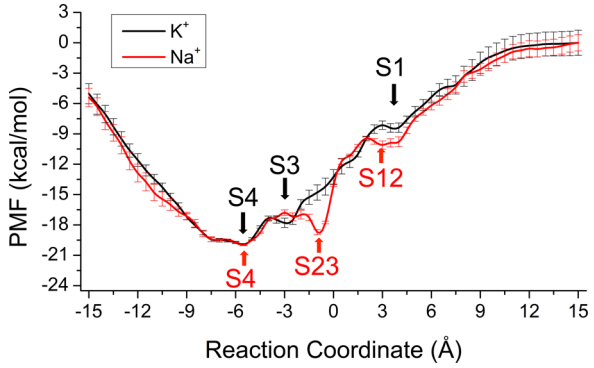

Figure 2. The 1D single-ion PMF for the movement of a single K^+ (black) or Na^+ (red) ion across the selectivity filter of NaK2CNG.

standard errors of the mean (presented by error bars in all figures) in this paper were calculated using the standard block-average calculations.[53] To check if other ions moved into the filter to affect sampling for permeant ion, the average number of ions within a confinement radius of 5 Å around the carbonyl oxygen of V63 was graphed in Supporting Information Figure S1. The effect of the contaminant ion on the computed PMFs was found to be insignificant.

In the PMF profile, there are three energy wells corresponding to the binding sites of S1, S3, and S4 for K^+. The energy wells for Na^+ correspond to the planar sites referred to here as S12, S23, and S4 in the filter as described previously. This coordination has been reported several times before for Na^+ binding to a selectivity filter of K^+ channel and was proposed to be energetically favorable, though kinetically unstable.[3,19,20,32] The ion binding sites found in the crystal structures (S2, S3, and S4) correlate to the locations of energy wells found in PMF computations. The widths of the binding wells suggest a broad distribution of possible ligation states for each ion. The 1D single-ion PMF computed for K^+ or Na^+ traversing the selectivity filter does not reveal any noticeable differences in the barriers or depths of the binding wells between the two ions. This finding is in good accord with reported nonselective monovalent cation transport for this mutant.

To investigate the effect of a multi-ion occupancy on the permeation of Na^+ and K^+ across the NaK2CNG channel, the free energy landscapes were computed for different occupancies of the channel. To verify the convergence of our sampling, 1D multi-ion PMFs from 2D PMF maps were tested and are shown in Supporting Information Figure S2. The convergence was reached after simulations of 125 ps. We considered several possible ion loads: K^+ ions ($K^+/K^+/K^+$), Na^+ ions ($Na^+/Na^+/Na^+$), and a mixed salt ($Na^+/K^+/K^+$), respectively. The 2D PMF maps in Figure 3A show that S1/S2/S4 occupancy for K^+ is the most stable. This is in contrast to the multidimensional PMFs for the narrow filter of KcsA reported by Egwolf and Roux which exhibit energy penalties for S1/S2/S4 load.[3] K^+ residing in site S1 (Figure 3A) retains its partial hydration. The binding of a monovalent cation to S1 is further promoted by the negatively charged carboxylate of D66. Noskov and Roux[20,22] noted that in reduced models of Na^+ or K^+ selective binding sites the presence of an additional carboxylate ligand is generally associated with a decrease in K^+ selectivity for models comprised of carbonyls, a single carboxylate, and varying number of water molecules.[23] The ability of the ion to retain most of its solvation shell also affects the K^+ selectivity of this site (S1). Na^+ binds preferentially to the sites S1, S23, and S4 in the Na^+-only condition (as shown in Figure 3B). If a mixture of ions is used (Figure 3C), Na^+ shows a tendency to bind to S1 (D66) while the middle K^+ ion occupies site S2 and the innermost site S4 holds K^+ in the mixture of ions.

To better illustrate the distribution of wells and barriers on the 2D maps, we computed one-dimensional multi-ion PMFs from the two-dimensional PMFs using the lowest energy path as described by Egwolf and Roux.[3] The resulting 1D multi-ion slices are shown in Figure 3D. The 1D multi-ion PMF slices show that the outer binding site can accommodate either K^+ or Na^+ (positions corresponding to that of site S1). Furthermore, the above PMF analyses show that there are no marked differences in binding energetics and barriers between the various monovalent cations. The multi-ion pore occupancy is essential to the "knock-out" permeation mechanism, but simultaneous occupancy of the selectivity filter by two or more ions does not affect its selectivity (or lack of thereof).

Potentials of Mean Force for Ion Permeation across the NaK2K Channel. PMFs for the K^+-selective NaK2K channel were also computed. The single-ion PMFs (shown in Figure 4) display five well-marked energy minima for K^+. These sites correspond to the binding sites S1, S2, S3, S4, and the external binding site S0. In contrast, there are only three well-defined binding sites for Na^+ in the positions S0, S2, and S34. Notably, the Na^+ ion has to overcome a high energy barrier to move between the S0 and S2 sites. The absence of the negatively charged residue (D/Y66) leads to a significant drop in ion hydration (see Discussion) and reduced attractive interactions with the channel. Therefore, a permeant cation feels an entry barrier for moving between S0 and S2 (for example Na^+ following the concentration gradient).

To investigate multi-ion effects, we extended the 2D PMF-based strategy to compare the ion permeation energy surface as function of monocationic (pure K^+ or Na^+) or mixed (both Na^+ and K^+ in the mixture) electrolyte solutions. The resulting PMFs are shown in Figure 5 A–C. For pure K^+ salt, three possible ion loads (configurations) in the filter were found

dx.doi.org/10.1021/jp4107537 | J. Phys. Chem. B 2014, 118, 2041–2049

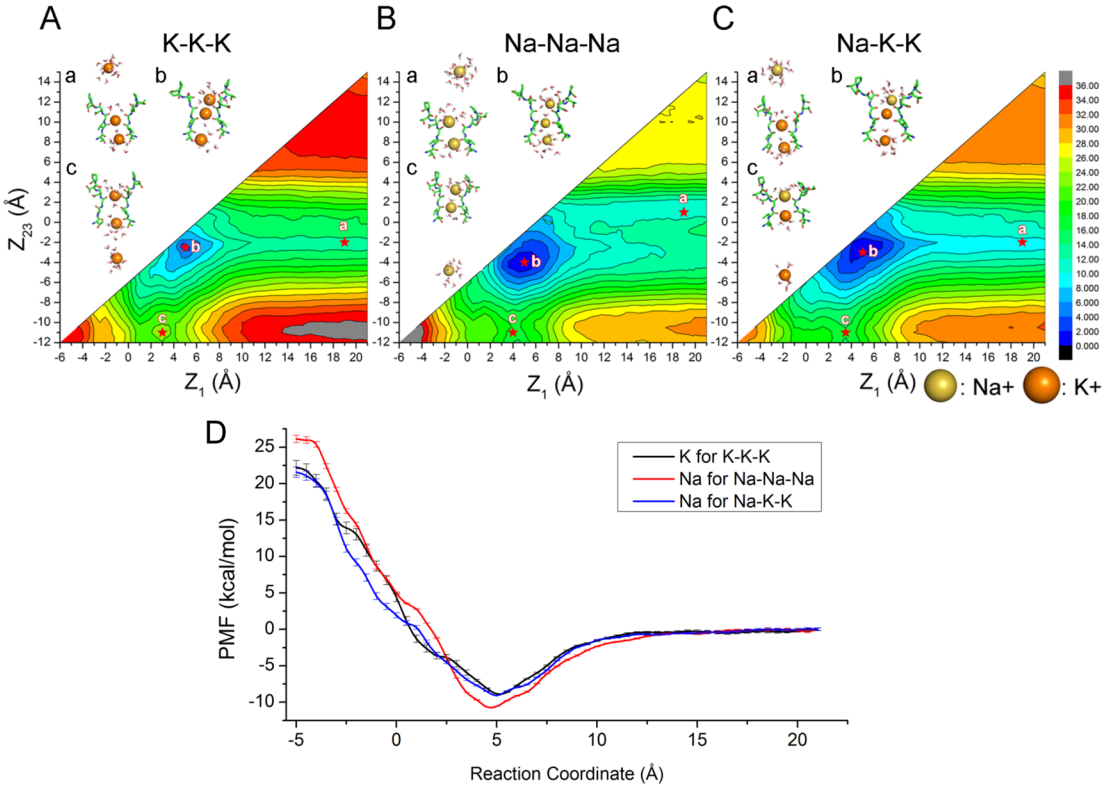

Figure 3. The 2D multi-ion PMFs for the movement of three ions with pure K^+ environment (A), pure Na^+ environment (B), and mixed environment (C) in the NaK2CNG channel. Contour lines are drawn every 2 kcal/mol. The configuration in the energy minima is displayed with red labeled points. K−K−K and Na−K−K describe the plots where a Na^+ or a K^+ ion moves in the presence of two K^+ ions. Na−Na−Na is the plot where Na^+ moves in the presence of two Na^+ ions. In every case, three ions were free to move, as indicated in the insets. (D) The 1D multi-ion PMFs for coordinate Z_1 calculated from 2D multi-ion PMFs for NaK2CNG channel, integrated from the multi-ion occupancy contour plots shown in (A−C). Each profile follows the lowest energy pathway across the corresponding 2D multi-ion PMF.

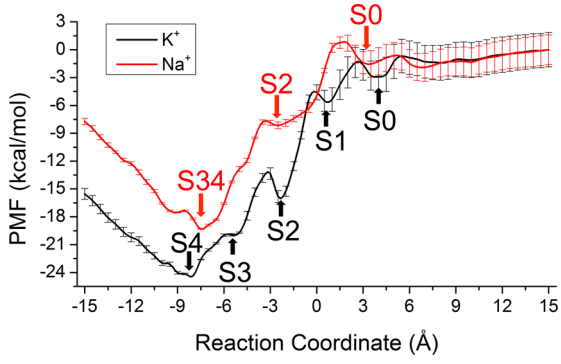

Figure 4. The 1D single-ion PMF for the movement of a single K^+ (black) or Na^+ (red) ion across the selectivity filter of NaK2K.

(Figure 5A). In the first, labeled as state ***a***, the two innermost K^+ ions occupy the sites S1 and S3, respectively. The outermost ion binds to a position near S0. In state ***b***, the two innermost K^+ bind to sites S2 and S4, while the outermost K^+ occupies S0. Finally, in state ***c*** the two outermost K^+ reside in S2 and S4, and the innermost K^+ moves into the cavity site. In the Na^+ solution, the free energy states as shown in Figure 5B are very similar to the binding position for K^+ in the filter shifted slightly. The shift in the position of the binding site for Na^+ has been discussed at length by Kim and Allen.[32] They concluded that Na^+ favors binding to a carbonyl plane with additional coordination by water molecules. This leads to the outer Na^+ in state ***a*** to bind to a S0-like position, while the two other Na^+ sites correspond to novel sites S12 and S34. This conformation was found to be the most stable when there are only two ions in the filter.[54] In the presence of a third ion the most stable configuration becomes state ***b*** where S01, S2, and S34 are occupied. In contrast, the binding sites in a filter occupied by a mixture of cations display notable differences as shown in Figure 5C. The most stable state has Na^+ located in site S12, while K^+ can be found in S3 and at the interface formed by the S4 carbonyls and water molecules in the intercellular cavity. This is a dominant state associated with larger penalties for ion translocation. Essentially, the outer Na^+ acts as a blocker at S12. Na^+ displays a deeper energy well compared to that of K^+ in the mixed filter occupancy. This is achieved by a combination of favorable ion-site interactions with a considerably smaller ion−ion repulsion compared to that of a Na^+−Na^+ pair occupying the filter. To illustrate an effective 1D PMF from a multi-ion map, we computed 1D multi-ion PMF slices. As shown in Figure 5D, for pure K^+ environment the free energy minima are located at S0 and S2. Also, there was a steep rise in PMF between sites S1 and S3. For Na^+ occupying the filter, the minima on the 1D multi-ion PMF slice is located between S0−S2.

Barriers and Dissociation Constants from PMFs. To illustrate the potential effect of an entry barrier to ion permeation across the filter we computed rate constants for ion permeation across this idealized potential of mean force (neglecting multi-ion effects). We employed Kramer's rate theory to estimate the characteristic time required for barrier crossing of an effective 1D potential using the 1D multi-ion

dx.doi.org/10.1021/jp4107537 | J. Phys. Chem. B 2014, 118, 2041−2049

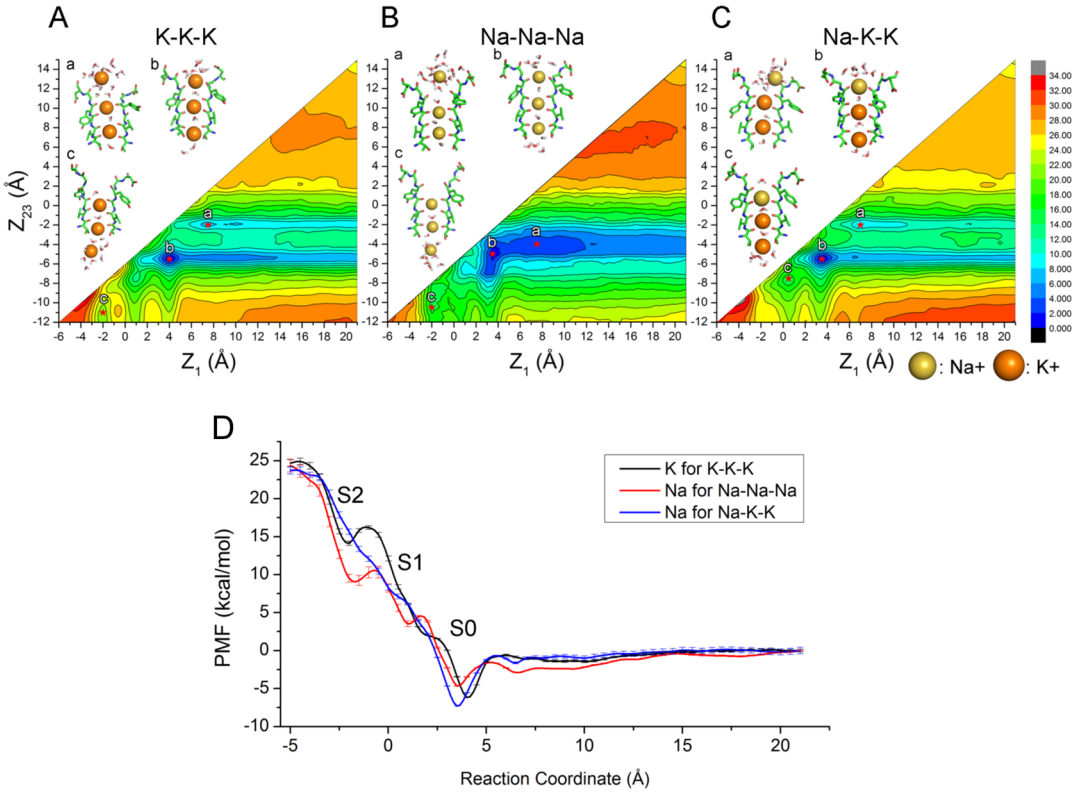

Figure 5. The 2D multi-ion PMFs for the movement of three ions in the NaK2K channel with pure K^+ environment (A), pure Na^+ environment (B), and mixed environment (C). Counter lines are drawn every 2 kcal/mol. The configuration in the energy minima is displayed with red labeled points, along the lowest energy permeation pathway. K−K−K and Na−K−K describe the plots where a Na^+, or a K^+ ion, moves in the presence of two K^+ ions. Na−Na−Na is the plot where Na^+ moves in the presence of two Na^+ ions. (D) The 1D multi-ion PMFs for coordinate Z_1 calculated from 2D multi-ion PMF for NaK2K channel, integrated from the multi-ion occupancy contour plots shown in (A−C).

PMF slices extracted from 2D multi-ion PMF computations. The results of these computations for different ions are collected in Supporting Information Table S1. The exact details of rate computations are well described by Kim and Allen.[32] We focus our computations only on the process of ion binding/escape from site S0 into bulk solution. The Kramer's rate for ion transfer from S0 to bulk is ∼0.0005, 0.002, and 0.12 ns^{-1} in mixed, K^+ only, and Na^+ only occupancies of the filter, respectively. The Na^+ captured in the filter along with two K^+ ions appears to be a potent blocker. The computed 1D multi-ion PMF profiles shown in Figure 5D allow us to compute the equilibrium dissociation constants as a function of ion loads of the filter. The data collected in Table 1 show that Na^+ can potentially bind to a filter provided that K^+ is a copermeant ion. However it cannot exit the filter once it enters. Interestingly, computed dissociation constants for ions in the filter agree reasonably with the ones estimated experimentally in 2013 by Liu and Lockless.[55] They reported binding affinities of K^+ and Na^+ to the NaK2K variant of NaK to be ∼54 ± 13 and 78 000 ± 12 000 μM, respectively. Liu and Lockless compared equilibrium binding affinities for a mixture of K^+ and Na^+ competing for the selectivity filter of NaK2K. The theoretical estimates from this study suggest the following equilibrium dissociation constants for K^+ and Na^+ in multi-ionic mixtures: 1070 and 8260 μM, underestimating relative affinities of K^+ versus Na^+. It is important to stress that this deficiency may only be partially related to the inaccuracy of the force fields that led to underestimating the selectivity of NaK2K. While the trend observed in the simulation is correct, K^+ is favored over Na^+ for example, the computed selectivity for K^+ is underestimated compared to that from experiment. The recent study of Lev et al. utilizing QM/MM free energy perturbation (FEP) simulations showed that Na^+/K^+ parameters used in CHARMM-27 provided accurate relative free energies comparable to that of high-level DFT free energy simulations.[56] One additional source for discrepancies in absolute numbers may be the implied stoichiometry of ion load in the filter during simulations. Liu and Lockless reported Hill coefficients for ion binding to selectivity filter of NaK2K of 1.4 ± 0.3. While it can be attributed to ion−ion interactions in the filter, it may also suggest that double ion occupancy of the filter is, obviously, an abstraction that does not capture all possible conductive states with one, two, or three ions in the filter. For example, in the case of single ion binding to the filter there is a clear 1000-fold difference between Na^+ and K^+ in NaK2K (Table 1), suggesting important roles played by equilibrium single-ion thermodynamics.[57] In addition to that, nonstoichiometric replacement of

Table 1. Equilibrium Dissociation Constants (EDC) and Gibbs Free Energies for Single- and Multi-Ion Occupancy from PMF Computations in NaK2K Channel

	EDC (mol/L)	ΔG (kcal/mol)
K^+	1.99×10^{-16}	−22.6
Na^+	1.67×10^{-13}	−17.4
K^+ in K−K−K	1.07×10^{-03}	−4.28
Na^+ in Na−Na−Na	8.26×10^{-03}	−3.00
Na^+ in Na−K−K	1.70×10^{-04}	−5.43

dx.doi.org/10.1021/jp4107537 | J. Phys. Chem. B 2014, 118, 2041−2049

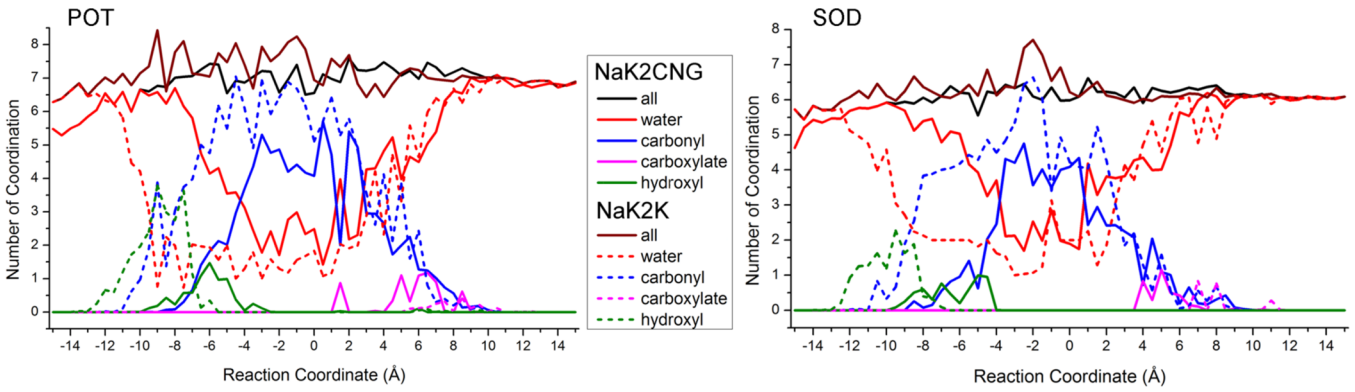

Figure 6. Average coordination numbers for K^+ or Na^+ ion in the transport process. The atoms coordinating K^+ or Na^+ ions were calculated from the 1D umbrella sampling simulations. A functional group was counted when the oxygen was less than 3.5 Å from the ion.

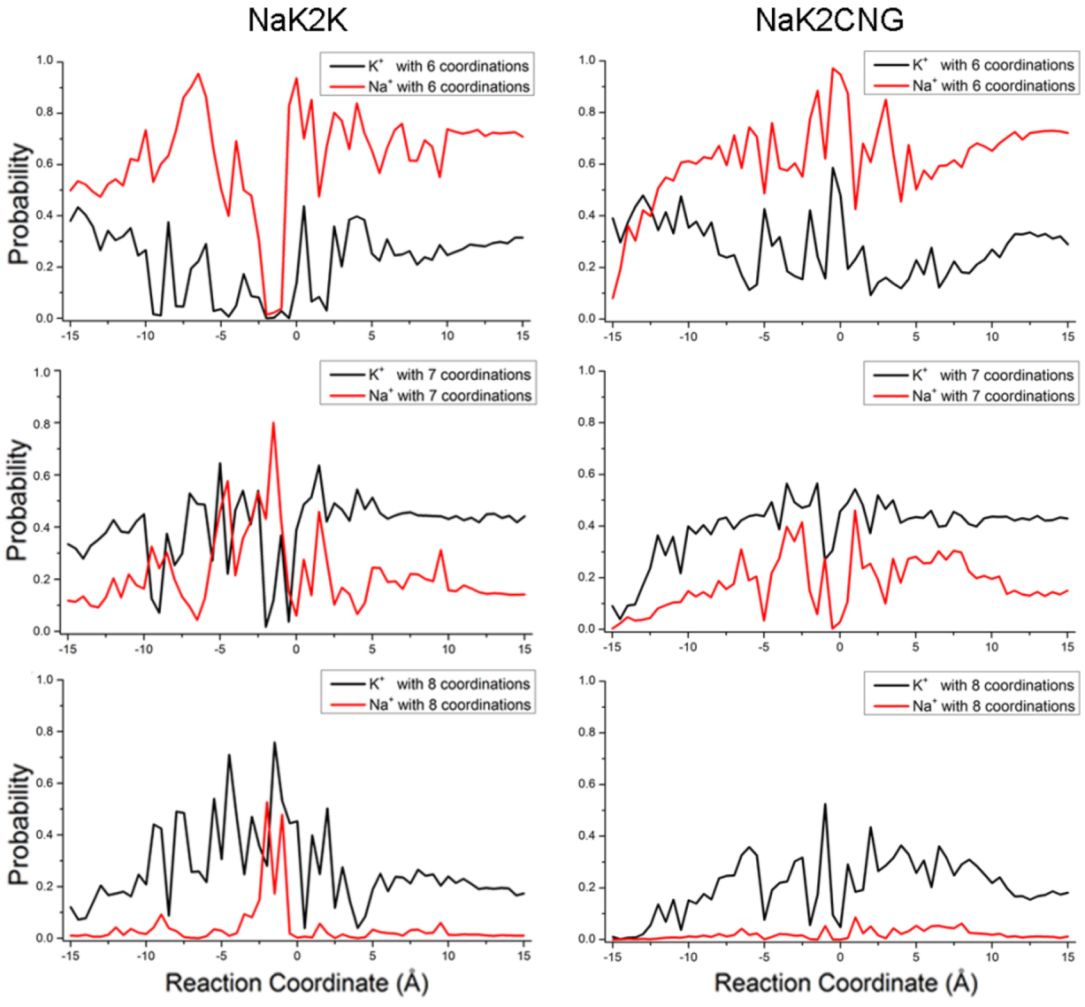

Figure 7. The probability of finding a given coordination number along the reaction coordinate (constrained ion positions along central axis of the channel) for selective pore (NaK2K) and nonselective pore (NaK2CNG).

K^+ by Na^+ during transport cycle may also add complexity in relating computed affinities to ones measured experimentally.

Selective Conductance and Site Hydration. A recent debate has highlighted the idea of an intimate relationship between ion coordination preferences in the bulk solution and the resultant selectivity. The factors which affect ion selectivity have been discussed including such topics as the number of coordinating ligands, the ligand dipole moment, the vibrational motion of the ligands and chemical type of the ligands.[12,58−61] It is important to mention, however, that most of the findings put forth in this debate use only reduced models of the selectivity filter of K-channels or Na^+-selective transporters and are focused mainly on the discussion of thermodynamic factors determining selective binding and single-ion occupancy. Several reports highlight possible limitations of such an approach in the case of K-channels, where kinetic effects are important.[32,45] In this paper, we have compared the differences and similarities between the coordination behavior of the selectivity filter in K^+-

dx.doi.org/10.1021/jp4107537 | J. Phys. Chem. B 2014, 118, 2041−2049

selective and nonselective channels and related them to barriers/wells observed in PMF. To simplify such a comparison we focused on single-ion PMF profiles where only one ion was moved along the permeation coordinate, while the environment around it was unconstrained. First, we identified the position-dependent ion coordination number for each ion for each window along the PMF reaction coordinate (as shown in Figure 6), where oxygens within a confinement radius of 3.5 Å around the ion were counted as coordinating. The choice of the confinement radius is based on the size of the coordination shell taken from our previous studies on ion hydration by aqueous clusters and model protein sites, where it was found to faithfully reproduce relative free energies.[22,56] The average coordination number of Na^+ and K^+ does not change substantially between selective and nonselective channels except for a small region located -1.0 Å $< z < -3.0$ Å corresponding to the center of site S2. This also corresponds to the region with the largest difference in well depth between K^+ and Na^+, $\Delta\Delta G(K^+/Na^+)$, which in the K-selective channel is ∼7−8 kcal/mol (see Figure 4).

Detailed FEP computations on the ion constrained at the center of this site for KcsA, reported by Kim and Allen, show that it is very selective.[32,45] However this begs the question why such a site is not observed in the nonselective channel NaK2CNG despite preservation of the GYG sequence and the apparent availability of the eight carbonyl oxygens needed to form the twisted coordination shell favored by K^+. Furthermore it leads one to wonder, what is the difference in ion coordination between the two channels? The set of umbrella-sampled windows from the PMF computations allow for testing of position-specific coordination numbers for each ion along the reaction path. While the distributions from biased simulations are not completely equivalent to equilibrium coordination states, they may still offer insight into solvent relaxation around the ion in different parts of the channel. The 1D single-ion PMF profile shown in Figure 2 shows that Na^+ does not reside in site S2, but binds at a location labeled S12. The ion bound to site S2 in the nonselective channel (NaK2CNG) has a higher count of water molecules with $N_{H2O} \sim 2.1-2.5$ compared to $N_{H2O} \sim 1.5-2.0$ in the NaK2K channel. The permeant ion retains more water in the "driest" area of the selectivity filter in a nonselective pore allowing for stable binding to S12. The average number of carbonyl groups involved in ion coordination in site S2 of a selective pore is 6.2 and 5.4 for K^+ and Na^+, respectively. A nonselective pore has 4.8 and 4.1 carbonyl oxygens involved in ion coordination in the most selective site. It is important to mention that in a nonselective channel, a carboxylate group can contribute to ion coordination essentially allowing efficient dehydration for both Na^+ and K^+ and transport through the most dehydrated part of the filter. Therefore, it can be concluded that dynamic changes in coordination environment and types of coordination groups are at play in the formation of selective binding site at the center of the selectivity filter. The additional binding site missing in NaK2CNG mutant allows for efficient dehydration and an increase in carbonyl involvement in bound ion stabilization.

Selective Conductance and Coordination Numbers. To illustrate the dynamics of coordination numbers along the reaction coordinate for an ion constrained in different positions across two channels, we computed probabilities of different ionic coordination states as a function of ion position along the reaction coordinate. A similar approach was used by Egwolf and Roux for analysis of coordination preferences in KcsA.[3] It is important to note that the harmonic restraint acting on the permeant cation does not bias the dynamics of the surrounding protein and water molecules. Figure 7 shows the probability profiles for the selective and nonselective channels for an ion constrained with a harmonic potential along the central axis of the channel, for example, corresponding to computed 1D PMFs. It is obvious that the coordination state displays some correlation with wells observed in PMF profiles for K^+ and Na^+. The "over-coordinated" states with $N > 6.5$ are present only in the most dehydrated part of the filter (-3 Å $< z < 1$ Å) for the selective channel. Yet other sites in the selectivity filter (S3 for example) display no overcoordination penalty ($N < 6$) for Na^+ but still remain selective for K^+ in the NaK2K channel and nonselective for either Na^+ or K^+ in NaK2CNG pore. This suggests that coordination number, while an important component of selective permeation, is insufficient for unambiguous predictions of ion selectivity in protein site and that other factors, such as chemical compositions are at play. Data collected in Figure 6 shows that carbonyl oxygens are the primary coordinating ligands for selective channel along the entire selectivity filter. NaK2CNG, on another hand, shows a steady increase in a hydration from $N = 2$ in the middle of site S2 to $N \sim 3-4$ in the adjacent sites. Accordingly, we conclude that chemical functionality of the selectivity filter, along with the dehydration patterns and presence of entrance barriers are true requirements for selective and efficient conductance. The ability to overcoordinate an ion plays an important role by providing an additional yet secondary contribution to the chemistry of ion selectivity in K-selective channels.

■ CONCLUSIONS

In this paper, we employed multiple methods to study the thermodynamical properties of the nonselective (NaK2CNG) and K-selective (NaK2K) variants of NaK channel ranging from standard MD simulations to multidimensional PMF mapping. The single-ion (1D) PMFs of the NaK2CNG channels display nearly identical profiles for K^+ and Na^+ ions. In contrast, the NaK2K channel shows significantly different energetics for K^+ and Na^+ permeation. The deep free-energy wells indicate that a single ion may bind too tightly to a selective filter for efficient permeation. Therefore multi-ionic effects must be accounted for to fully understand ion transport across NaK channels variants. To study effects of copermeant ions we performed a series of 2D PMF computations. In the free energy landscapes of the NaK2CNG channel with three different conditions, there are similar free energy minima configurations. The existence of negatively charged carboxylate of D66 decreases the K^+ selectivity of NaK2CNG channel. Meanwhile, the integrated one-dimensional PMFs show no marked differences in binding energetics or barriers. This is reminiscent of the mutant NavAb channel from the bacterium *Arcobacter Butzleri* where the channel loses the selectivity by losing well-defined binding sites with a conservative mutation where glutamates are replaced by aspartates.[62,63] Conversely, the free energy maps with three different conditions are unique in the NaK2K channel. There were stable configurations with the inner ion present in the cavity in the pure K^+ or Na^+ condition. The outer Na^+ ion may produce a blockade of the filter in the presence of K^+.

As Furini et al.[19,64] proposed, in the boundary between S2 and S3 in NaK2CNG channel, Na^+ can be perfectly surrounded by an octahedral coordination shell (six coordinates with four oxygen atoms from the protein residues and two from the water

dx.doi.org/10.1021/jp4107537 | J. Phys. Chem. B 2014, 118, 2041−2049

molecules) with three binding sites. Meanwhile, a carboxylate group also assists in coordinating ions and dehydrating the environment of ions. By contrast, the environment differs in the NaK2K channel with four binding sites. In keeping with our previous studies, the presence of a high-field ligand is essential for reducing preference of a system for K^+. This dynamic shell arrangement is impossible for the analogous site S2 in the K^+ selective NaK2K channel. The permeant ion has to be essentially dehydrated in the site and coordinated predominantly by carbonyl groups, which is not the case for a nonselective variant. The number of coordinating ligands also plays a role in the formation of K-selective permeation. While this work like many other computations of ion permeation depends on a quality of force-fields used,[21,65] previous studies of monovalent cation transport performed with polarizable[66,67] and quantum mechanics potential functions[56] show that classical force fields are qualitatively correct.

■ ASSOCIATED CONTENT

Ⓢ Supporting Information

Figures S1 and S2 illustrate time series of ion occupancies in the selectivity filter and convergence of PMF computations, respectively. Table S1 presents transition times for ion transfers between sites. This material is available free of charge via the Internet at http://pubs.acs.org.

■ AUTHOR INFORMATION

Corresponding Author

*E-mail: snoskov@ucalgary.ca.

Author Contributions

[†]Y.W. and A.C.C. contributed equally.

Notes

The authors declare no competing financial interest.

■ ACKNOWLEDGMENTS

The discussions of the transport mechanisms with Drs. I. Vorobyov and P. Tieleman are greatly acknowledged. We also acknowledge the discussions on the multidimensional PMFs with Dr. T. W. Allen. We would like to acknowledge financial support from the Natural Sciences and Engineering Research Council (NSERC) Discovery grant program (RGPIN 340946-07) and a Resource Allocation Award from WestGrid, Canada. S.N. is an Alberta Innovates Technology Futures New Faculty.

■ REFERENCES

(1) Sansom, M. S. P. Ion channels: Structure of a molecular brake. *Curr. Biol.* **1999**, *9*, R173−R175.

(2) Sontheimer, H. An unexpected role for ion channels in brain tumor metastasis. *Exp. Biol. Med.* **2008**, *233*, 779−791.

(3) Egwolf, B.; Roux, B. Ion selectivity of the KcsA channel: a perspective from multi-ion free energy landscapes. *J. Mol. Biol.* **2010**, *401*, 831−842.

(4) Doyle, D. A.; Cabral, J. M.; Pfuetzner, R. A.; Kuo, A. L.; Gulbis, J. M.; Cohen, S. L.; Chait, B. T.; MacKinnon, R. The structure of the potassium channel: Molecular basis of K^+ conduction and selectivity. *Science* **1998**, *280* (5360), 69−77.

(5) Jiang, Y. X.; Lee, A.; Chen, J. Y.; Ruta, V.; Cadene, M.; Chait, B. T.; MacKinnon, R. X-ray structure of a voltage-dependent K^+ channel. *Nature* **2003**, *423* (6935), 33−41.

(6) Kuo, A. L.; Gulbis, J. M.; Antcliff, J. F.; Rahman, T.; Lowe, E. D.; Zimmer, J.; Cuthbertson, J.; Ashcroft, F. M.; Ezaki, T.; Doyle, D. A. Crystal structure of the potassium channel KirBac1.1 in the closed state. *Science* **2003**, *300* (5627), 1922−1926.

(7) Brohawn, S. G.; del Marmol, J.; MacKinnon, R. Crystal Structure of the Human K2P TRAAK, a Lipid- and Mechano-Sensitive K(+) Ion Channel. *Science* **2012**, *335* (6067), 436−441.

(8) Zhao, C. F.; Noskov, S. Y. The Molecular Mechanism of Ion-Dependent Gating in Secondary Transporters. *PLoS Comp. Biol.* **2013**, *9*, e1003296.

(9) Larsson, H. P.; Wang, X. Y.; Lev, B.; Baconguis, I.; Caplan, D. A.; Vyleta, N. P.; Koch, H. P.; Diez-Sampedro, A.; Noskov, S. Y. Evidence for a third sodium-binding site in glutamate transporters suggests an ion/substrate coupling model. *Proc. Natl. Acad. Sci. U.S.A.* **2010**, *107*, 13912−13917.

(10) Doyle, D. A.; Morais Cabral, J.; Pfuetzner, R. A.; Kuo, A.; Gulbis, J. M.; Cohen, S. L.; Chait, B. T.; MacKinnon, R. The structure of the potassium channel: molecular basis of K^+ conduction and selectivity. *Science* **1998**, *280*, 69−77.

(11) Morais-Cabral, J. H.; Zhou, Y.; MacKinnon, R. Energetic optimization of ion conduction rate by the K^+ selectivity filter. *Nature* **2001**, *414*, 37−42.

(12) Noskov, S. Y.; Berneche, S.; Roux, B. Control of ion selectivity in potassium channels by electrostatic and dynamic properties of carbonyl ligands. *Nature* **2004**, *431*, 830−834.

(13) Berneche, S.; Roux, B. Energetics of ion conduction through the K^+ channel. *Nature* **2001**, *414*, 73−77.

(14) Berneche, S.; Im, W.; Roux, B. Ion conduction through the K^+ channel occurs via a knock-on mechanism. *Biophys. J.* **2002**, *82* (1), 206a−206a.

(15) Aqvist, J.; Luzhkov, V. Ion permeation mechanism of the potassium channel. *Nature* **2000**, *404*, 881−884.

(16) Luzhkov, V. B.; Aqvist, J. K^+/Na^+ selectivity of the KcsA potassium channel from microscopic free energy perturbation calculations. *Biochim. Biophys. Acta, Prot. Struct.* **2001**, *1548*, 194−202.

(17) Roux, B.; MacKinnon, R. The cavity and pore helices the KcsA K^+ channel: Electrostatic stabilization of monovalent cations. *Science* **1999**, *285*, 100−102.

(18) Zhou, Y.; Morais-Cabral, J. H.; Kaufman, A.; MacKinnon, R. Chemistry of ion coordination and hydration revealed by a K^+ channel-Fab complex at 2.0 A resolution. *Nature* **2001**, *414*, 43−8.

(19) Furini, S.; Domene, C. Nonselective Conduction in a Mutated NaK Channel with Three Cation-Binding Sites. *Biophys. J.* **2012**, *103*, 2106−2114.

(20) Noskov, S. Y.; Roux, B. Importance of hydration and dynamics on the selectivity of the KcsA and NaK channels. *J. Gen. Physiol.* **2007**, *129*, 135−143.

(21) Roux, B.; Berneche, S.; Egwolf, B.; Lev, B.; Noskov, S. Y.; Rowley, C. N.; Yu, H. B. Ion selectivity in channels and transporters. *J. Gen. Physiol.* **2011**, *137*, 415−426.

(22) Yu, H. B.; Noskov, S. Y.; Roux, B. Two mechanisms of ion selectivity in protein binding sites. *Proc. Natl. Acad. Sci. U.S.A.* **2010**, *107*, 20329−20334.

(23) Yu, H. B.; Noskov, S. Y.; Roux, B. Hydration Number, Topological Control, and Ion Selectivity. *J. Phys. Chem. B* **2009**, *113*, 8725−8730.

(24) Thomas, M.; Jayatilaka, D.; Corry, B. An Entropic Mechanism of Generating Selective Ion Binding in Macromolecules. *PLoS Comput. Biol.* **2013**, *9*, e1002914.

(25) Varma, S.; Rempe, S. Tuning ion coordination preferences to enable selective permeation. *Biophys. J.* **2007**, 1093−1099.

(26) Varma, S.; Rogers, D. M.; Pratt, L. R.; Rempe, S. B. Perspectives on: Ion selectivity Design principles for K^+ selectivity in membrane transport. *J. Gen. Physiol.* **2011**, *138*, 279−279.

(27) Varma, S.; Sabo, D.; Rempe, S. B. K^+/Na^+ selectivity in K channels and valinomycin: Over-coordination versus cavity-size constraints. *J. Mol. Biol.* **2008**, *376*, 13−22.

(28) Bostick, D. L.; Brooks, C. L. Selective Complexation of K^+ and Na^+ in Simple Polarizable Ion-Ligating Systems. *J. Am. Chem. Soc.* **2010**, *132* (38), 13185−13187.

(29) Bostick, D. L.; Brooks, C. L. Statistical determinants of selective ionic complexation: ions in solvent, transport proteins, and other "hosts". *Biophys. J.* **2010**, *98* (8), 1722−1722.

(30) Bostick, D. L.; Brooks, C. L. Selectivity in K^+ channels is due to topological control of the permeant ion's coordinated state. *Proc. Natl. Acad. Sci. U.S.A.* **2007**, *104*, 9260−9265.
(31) Thomas, M.; Jayatilaka, D.; Corry, B. How does over-coordination create ion selectivity? *Biophys. Chem.* **2013**, *172*, 37−42.
(32) Kim, I.; Allen, T. W. On the selective ion binding hypothesis for potassium channels. *Proc. Natl. Acad. Sci. U.S.A.* **2011**, *108*, 17963−8.
(33) Alam, A.; Jiang, Y. X. Structural analysis of ion selectivity in the NaK channel. *Nat. Struct. Mol. Biol.* **2009**, *16*, 35−41.
(34) Shi, N.; Ye, S.; Alam, A.; Chen, L. P.; Jiang, Y. X. Atomic structure of a Na^+- and K^+-conducting channel. *Nature* **2006**, *440*, 570−574.
(35) Derebe, M. G.; Sauer, D. B.; Zeng, W.; Alam, A.; Shi, N.; Jiang, Y. Tuning the ion selectivity of tetrameric cation channels by changing the number of ion binding sites. *Proc. Natl. Acad. Sci. U.S.A.* **2011**, *108* (2), 598−602.
(36) Gang, H.; Zhang, S. Na+ permeation and block of hERG potassium channels. *J. Gen. Physiol.* **2006**, *128*, 55−71.
(37) Jo, S.; Kim, T.; Iyer, V. G.; Im, W. CHARMM-GUI: a web-based graphical user interface for CHARMM. *J. Comput. Chem.* **2008**, *29* (11), 1859−1865.
(38) Brooks, B. R.; Bruccoleri, R. E.; Olafson, B. D.; States, D. J.; Swaminathan, S.; Karplus, M. CHARMM - a Program for Macromolecular Energy, Minimization, and Dynamics Calculations. *J. Comput. Chem.* **1983**, *4*, 187−217.
(39) MacKerell, A. D.; Bashford, D.; Bellott, M.; Dunbrack, R. L.; Evanseck, J. D.; Field, M. J.; Fischer, S.; Gao, J.; Guo, H.; Ha, S.; Joseph-McCarthy, D.; Kuchnir, L.; Kuczera, K.; Lau, F. T. K.; Mattos, C.; Michnick, S.; Ngo, T.; Nguyen, D. T.; Prodhom, B.; Reiher, W. E.; Roux, B.; Schlenkrich, M.; Smith, J. C.; Stote, R.; Straub, J.; Watanabe, M.; Wiorkiewicz-Kuczera, J.; Yin, D.; Karplus, M. All-atom empirical potential for molecular modeling and dynamics studies of proteins. *J. Phys. Chem. B* **1998**, *102*, 3586−3616.
(40) Feller, S. E.; MacKerell, A. D. An improved empirical potential energy function for molecular simulations of phospholipids. *J. Phys. Chem. B* **2000**, *104*, 7510−7515.
(41) Noskov, S. Y.; Roux, B. Control of ion selectivity in LeuT: Two Na(+) binding sites with two different mechanisms. *J. Mol. Biol.* **2008**, *377*, 804−818.
(42) Hoover, W. G. Canonical dynamics: Equilibrium phase-space distributions. *Phys. Rev. A* **1985**, *31*, 1695−1697.
(43) Essmann, U.; Perera, L.; Berkowitz, M. L.; Darden, T.; Lee, H.; Pedersen, L. G.; Smooth, A. Particle Mesh Ewald Method. *J. Chem. Phys.* **1995**, *103* (19), 8577−8593.
(44) Ryckaert, J.-P.; Ciccotti, G.; Berendsen, H. J. C. Numerical integration of the cartesian equations of motion of a system with constraints: molecular dynamics of n-alkanes. *J. Comput. Phys.* **1977**, *23*, 327−341.
(45) Thompson, A. N.; Kim, I.; Panosian, T. D.; Iverson, T. M.; Allen, T. W.; Nimigean, C. M. Mechanism of potassium-channel selectivity revealed by Na^+ and Li^+ binding sites within the KcsA pore. *Nat. Struct. Mol. Biol.* **2009**, *16*, 1317−U143.
(46) Kumar, S.; Bouzida, D.; Swendsen, R. H.; Kollman, P. A.; Rosenberg, J. M. The Weighted Histogram Analysis Method for Free-Energy Calculations on Biomolecules 0.1. The Method. *J. Comput. Chem.* **1992**, *13*, 1011−1021.
(47) Grossfield, A. *WHAM: the weighted histogram analysis method*, version 2.0.6; University of Rochester Medical Center: Rochester, NY, USA, 2012.
(48) Hänggi, P.; Talkner, P.; Borkovec, M. Reaction-rate theory: fifty years after Kramers. *Rev. Mod. Phys.* **1990**, *62* (2), 251−341.
(49) Crouzy, S.; Woolf, T. B.; Roux, B.; Molecular-Dynamics, A. Study of Gating in Dioxolane-Linked Gramicidin-A Channels. *Biophys. J.* **1994**, *67* (4), 1370−1386.
(50) Mamonov, A. B.; Kurnikova, M. G.; Coalson, R. D. Diffusion constant of K^+ inside Gramicidin A: A comparative study of four computational methods. *Biophys. Chem.* **2006**, *124* (3), 268−278.
(51) Allen, T. W.; Andersen, O. S.; Roux, B. Energetics of ion conduction through the gramicidin channel. *Proc. Natl. Acad. Sci. U.S.A.* **2004**, *101* (1), 117−22.
(52) Li, Y. H.; Andersen, O. S.; Roux, B. Energetics of Double-Ion Occupancy in the Gramicidin A Channel. *J. Phys. Chem. B* **2010**, *114*, 13881−13888.
(53) Rapaport, D. C. *The Art of Molecular Dynamics Simulation*, 2nd ed.; Cambridge University Press: Cambridge, 2004; pp iv−86.
(54) Shen, R.; Guo, W. L. Mechanism for Variable Selectivity and Conductance in Mutated NaK Channels. *J. Phys. Chem. Lett.* **2012**, *3*, 2887−2891.
(55) Liu, S. A.; Lockless, S. W., Equilibrium selectivity alone does not create K^+-selective ion conduction in K^+ channels. *Nat. Commun.* **2013**, *4*.
(56) Lev, B.; Roux, B.; Noskov, S. Y. Relative Free Energies for Hydration of Monovalent Ions from QM and QM/MM Simulations. *J. Chem. Theory Comput.* **2013**, *9*, 4165−4175.
(57) Liu, S. A.; Bian, X. L.; Lockless, S. W. Preferential binding of K+ ions in the selectivity filter at equilibrium explains high selectivity of K + channels. *J. Gen. Physiol.* **2012**, *140* (6), 671−679.
(58) Thomas, M.; Jayatilaka, D.; Corry, B. Mapping the Importance of Four Factors in Creating Monovalent Ion Selectivity in Biological Molecules. *Biophys. J.* **2011**, *100* (1), 60−69.
(59) Dixit, P. D.; Merchant, S.; Asthagiri, D. Ion Selectivity in the KcsA Potassium Channel from the Perspective of the Ion Binding Site. *Biophys. J.* **2009**, *96* (6), 2138−2145.
(60) Thomas, M.; Jayatilaka, D.; Corry, B. The predominant role of coordination number in potassium channel selectivity. *Biophys. J.* **2007**, *93* (8), 2635−2643.
(61) Dudev, T.; Lim, C. Competition among Ca^{2+}, Mg^{2+}, and Na^+ for model ion channel selectivity filters: determinants of ion selectivity. *J. Phys. Chem. B* **2012**, *116* (35), 10703−10714.
(62) Payandeh, J.; Scheuer, T.; Zheng, N.; Catterall, W. A. The crystal structure of a voltage-gated sodium channel. *Nature* **2011**, *475*, 353−358.
(63) Finol-Urdaneta, R. K.; Wang, Y.; Al-Sabi, A.; Zhao, C.; Noskov, S. Y.; French, R. J. Sodium channel selectivity and conduction: Prokaryotes have devised their own molecular strategy. *J. Gen. Physiol.* **2014**, *143* (2), 157−171.
(64) Furini, S.; Domene, C. Gating at the Selectivity Filter of Ion Channels that Conduct Na^+ and K^+ Ions. *Biophys. J.* **2011**, *101* (7), 1623−1631.
(65) Joung, I. S.; Cheatham, T. E. Determination of Alkali and Halide Monovalent Ion Parameters for Use in Explicitly Solvated Biomolecular Simulations. *J. Phys. Chem. B* **2008**, *112* (30), 9020−9041.
(66) Lev, B.; Noskov, S. Y. Role of protein matrix rigidity and local polarization effects in the monovalent cation selectivity of crystallographic sites in the Na-coupled aspartate transporter Glt(Ph). *Phys. Chem. Chem. Phys.* **2013**, *15* (7), 2397−2404.
(67) Illingworth, C. J. R.; Furini, S.; Domene, C. Computational Studies on Polarization Effects and Selectivity in K+ Channels. *J. Chem. Theory Comput.* **2010**, *6* (12), 3780−3792.